

Differences of Cations and Anions: Their Hydration, Surface Adsorption, and Impact on Water Dynamics

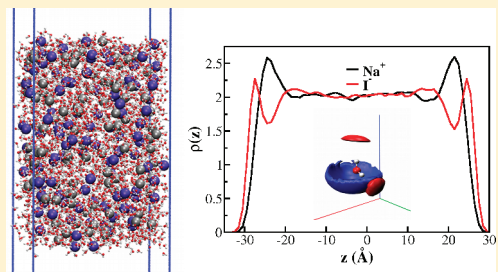
Lijiang Yang,[†] Yubo Fan,[‡] and Yi Qin Gao^{*,†}

[†]College of Chemistry and Molecular Engineering, Beijing National Laboratory for Molecular Sciences, Peking University, Beijing 100871, China

[‡]Department of Systems Medicine & Bioengineering, The Methodist Hospital Research Institute, Weill Cornell Medical College, 6670 Bertner Avenue, Houston, Texas 77030, United States

 Supporting Information

ABSTRACT: The higher tendency for anions to accumulate at the salt aqueous solution/air interface than that of cations has been observed experimentally and theoretically, suggesting that the size and polarizability of the ions play essential roles in this effect. Here, we investigate the influence of the nonsymmetrical positive-vs-negative charge distribution in water molecules to the hydration and surface/bulk partition of the solvated positively and negatively charged particles by using molecular dynamics simulations with hypothetical ions to validate our theoretical models. The results indicate that positive and negative charges (called cations and anions, respectively, although they may not really exist in experiments) with all other properties identical are hydrated differently and that the anions are more likely to populate at the surface. The simulation on a combination series of cations and anions in aqueous solution shows significant variations on water dynamics, likely due to the specific cooperativity between oppositely charged ions.



1. INTRODUCTION

The water/air interface plays important roles in many areas including chemical, material, biological, and environmental sciences.^{1,2} One of the interesting physicochemical questions is on understanding how electrolytes such as inorganic salts affect the interfacial structures and how they are distributed near the interfaces. Such studies are at a central position in understanding the effects of salts on interfacial tension, surface stability, and the solubility of organic and biomolecules, as well as surface chemical reactions.^{3–6} In recent years, a large number of studies have been performed to investigate the binding of ions at water interfaces.^{5–24} One of the pioneering theoretical studies was done by Jungwirth and Tobias,^{5,16} who showed that anions, especially the large and highly polarizable ones, are preferred over cations at these interfaces. Their predictions were subsequently verified by the experiments of Saykally and co-workers.²¹ Different proposals were invoked to explain this phenomenon, which include size effects and polarizability.^{20,25}

However, classical molecular dynamics (MD) simulations on the water/air interface showed that the dipole of water molecules also slightly point into the vapor phase.^{26,27} In a recent study, we used molecular dynamics simulations combined with a simple statistical mechanical model to rationalize such an observation. It was shown that the charge distribution of the water molecular model plays an essential role in determining the orientation of water molecules at the water/air interface.²⁸ The water/air interface calculated^{29,30} using SPC/E water models yields a

surface electric potential of -0.55 V (the surface potential calculated using quantum chemistry/DFT methods, however, is positive; the inconsistency in quantifying the surface potential at the liquid–vapor interface when using explicit ab initio electronic charge density and effective atomic partial charge models of liquid water was resolved by Kathmann et al. recently³⁰). The classical studies suggest that the charge distribution of water may affect differently its interaction with positive and negative charges. Indeed, without including polarizability, positively and negatively charged but otherwise identical particles were found in MD simulations³¹ to occupy the surface of water droplets with different propensity: consistent with other studies with more realistic ion models, negatively charged particles have a higher tendency to be found at the interface than the positively charged ones. Furthermore, when MD simulations were performed for SPC/E water confined between two oppositely charged plates, wetting of the two otherwise identical surfaces depends heavily on the charge type assigned to them.³² Compared to that of neutral surfaces, positive charges increase and negative charges decrease water affinity to the model plates.

These results suggest that the intrinsic water charge distribution (in particular, with negative charges located on the oxygen atom and near the center of the molecule and the positive charges more on the periphery of the molecule) could play an important

Received: May 13, 2011

Revised: September 28, 2011

Published: September 29, 2011

Table 1. Force Field Parameters for Water Models

model	type	r_0 (Å) ^a	ϵ (kcal/mol)	r_1 (Å)	r_2 (Å)	q_1 (e)	q_2 (e)	θ (deg)	φ (deg)
SPC/E	A	1.7767	0.1553	1.0000		0.4238	-0.8476	109.47	
TIPSP	B	1.7510	0.160	0.9572	0.70	0.241	-0.241	104.52	109.47
POL3	A	1.798	0.156	1.0000		0.365	-0.730	109.47	

^a The van der Waals potential used in this study is $E_{VDW} = \epsilon[(r_0/r)^{12} - 2(r_0/r)^6]$.

Table 2. Force Field Parameters for Monovalent Ions

type	model	r_0 (Å)	ϵ (kcal/mol)	model	r_0 (Å)	ϵ (kcal/mol)
Li ⁺	Cheatham	0.791	0.3367344	Chang	N/A	N/A
Na ⁺		1.212	0.3526418		1.275	0.10
Cl ⁻		2.711	0.0127850		2.435	0.10
I ⁻		2.919	0.0427845		N/A	N/A

role in affecting water interactions with charged particles and surfaces. Bearing this in mind, in this simple study, we perform MD simulations for charges solvated in water. The purpose of this study is to analyze in detail the difference between the hydration of cations and anions. To avoid complexity brought in by the different aspects of ions, such as the size and polarizability, we mainly focus on using nonpolarizable models and use both more realistic ion models such as Li⁺ + I⁻ as well as fake ionic systems in which cations and anions are of the same size and have the same van der Waals interaction parameters. Here, we note that the current study is aiming at a simplified and qualitative understanding of the effects of charge signs on hydration, the force fields used are probably very approximate, and that the ion models are given their names in the text only for convenience but not for their real physical properties.

The article is organized as follows: in the section 2, we provide the details of the simulations and in section 3, the calculated results are presented. The results are discussed in section 4.

2. COMPUTATIONAL METHODS

In this study, the SPC/E water model and refitted monovalent ion parameters for the Ewald and SPC/E (Table 1,2) water models from Cheatham et al. were employed.³³ Besides the alkali (Li⁺, Na⁺) and halide (I⁻, Cl⁻) ions, fake ions (Li⁻, Na⁻, I⁺, and Cl⁺), which have the same van der Waals parameter as the normal ones, are also used. In order to test the effect of point charge distributions and polarizability on the hydration of ions, we also performed MD simulations using the TIPSP water model³⁴ and the POL3³⁵ polarizable force field (Table 1) for the I⁻I⁻ system. In the simulations using the polarizable water model, Dang-Chang^{36,37} monovalent ion parameters are employed (Table 2). All simulations were performed using the AMBER9 molecular dynamics package.³⁸ A rectangular box was created with 2700 water molecules and 105 cations/anions (which correspond to a concentration of 2 M). The particle-mesh Ewald

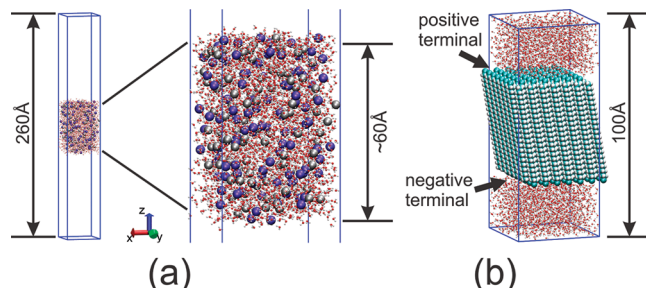


Figure 1. (a) Rectangular water/ion solution slab with two air/liquid interfaces being at the top and bottom, respectively; (b) water confined by linear *n*-tetracontane single molecule film (the whole system is shifted by 50 Å by the *z*-dimension to position the water film in the middle of the box when analyzing the collected data in the trajectories).

method³⁹ with a real space cutoff of 10 Å was used to treat long-range electrostatic interactions. The SHAKE algorithm with a relative geometric tolerance of 10⁻⁸ was used to constrain all bonds, including hydrogen, and all dynamics calculations utilized a 2 fs time step.

To obtain a reasonable initial structure, a 20 ps MD simulation was first performed to heat the system from 0 to 360 K, followed by a 200 ps equilibration at 360 K and 1 atm. Next, the system was cooled to 300 K by another 20 ps MD simulation followed by a 1 ns equilibration at 300 K and 1 atm. The resulted final box size was approximately 40 × 40 × 60 Å³. In the second step, the *z*-dimension was increased by 200 Å, while the *x*- and *y*-dimensions were kept intact (that is at a 40 × 40 × 260 Å³ rectangular box) resulting in a column geometry containing two air/water interfaces (Figure 1a). Starting from the configuration obtained from the last frame of the NPT calculation, all of the calculations in this step were carried out under the NVT ensemble to maintain the two air/water interfaces at the top and bottom sides of the water slab. All the water/ion solution slabs were simulated for 100 ns, and the last equilibrated 50 ns trajectories were collected and analyzed.

To investigate the influence of charged surfaces on water structure and dynamics, systems with a single molecule film containing 98 *n*-tetracontanes and 2642 water molecules were constructed, as seen in Figure 1b. The alkane chains are tilted by 33.85° from the *z*-direction. Three hydrogens on one terminal of the linear alkanes were removed, and charges were assigned to

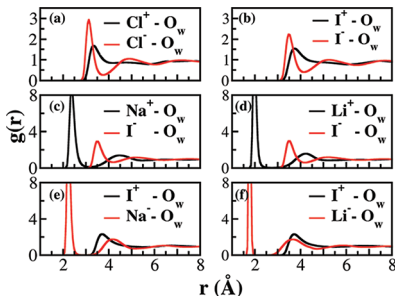


Figure 2. RDF of water surrounding the ions in the systems, including (a) Cl^+Cl^- , (b) I^+I^- , (c) NaI , (d) LiI , (e) I^+Na^- , and (f) I^+Li^- .

these naked carbon atoms, while all other atoms were set neutral. Forty-nine of them were assigned as positively charged on the terminal and the rest of the 49 as negatively charged ones. The charge amount was set as 0, 0.1, 0.2, 0.4, 1, and 5 in six systems. Each of the next alkanes with the same charged terminals are 5.7 Å apart in the x - or y -directions, while they are identical in z -direction. The charged alkanes are in the center of the square formed by four oppositely charged alkanes on the xy plane. The water layer was previously equilibrated at 300 K and 1 atm, and its size was adjusted to match the alkane film before the assembling of the alkane and water layers. Thus, the primary cell was constructed as a box with $\sim 40 \times 40 \times 100$ Å³. All alkane atoms were kept fixed during the simulation under 300 K and constant volume. All systems were run for 10 ns, and the last 5 ns trajectories were collected for analysis.

It is well-known that the truncation of Lennard-Jones interactions influences different properties of liquids to various extents.⁴⁰ Therefore, corrections due to the truncation of dispersion interactions in the simulations of homogeneous systems are proposed.⁴¹ Janecek et al. also discussed the corrections in inhomogeneous systems (such as at an interface).⁴² In this study, the systems we are interested in are aqueous solutions containing ions. It is found that in these systems, the electrostatic forces are several orders higher than the dispersion forces, and the behavior of such systems is not considerably affected by the improper treatment or neglect of the long-range contributions due to truncated dispersion interactions.⁴³ However, in order to make sure that the cutoff of 10 Å used in this study does not induce artifacts, another simulation that employed a larger cutoff of 13 Å for the I^+I^- /water solution slab was conducted for 100 ns. Through comparing the ion–water radial distribution functions, the ion density profiles, and the rotational relaxation of water molecules with those results calculated from the simulations with the cutoff of 10 Å, we found that the cutoff of 10 Å is large enough for the studies in this work (the comparisons of the RDFs, the density profiles, and the rotational relaxation of water molecules can be found in the Figures S1, S2, and S3, respectively, of the Supporting Information). Another factor that might affect the results of our simulations is the lattice spacing used in the Ewald summations. A value of 1 Å was employed in our studies. In order to check if our choice of the lattice spacing was adequate, another 100 ns simulation using a rather small lattice spacing of 0.5 Å was conducted for the LiI/water solution. The similarities of the results of the two simulations, lattice spacing of 1 Å and 0.5 Å, showed that the lattice spacing of 1 Å is a reasonable choice (the corresponding comparisons can be found in the Figures S4, S5, and S6 of the Supporting Information).

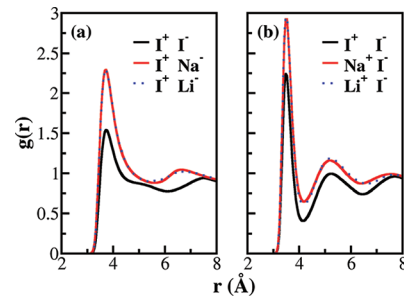


Figure 3. Effects of counterions on the hydration of selected ions. The RDF for water surrounding (a) I^+ , in the presence of I^- , Na^- , and Li^- ; and (b) I^- , in the presence of I^+ , Na^+ , and Li^+ .

3. RESULTS

3.1. Water Radial Distribution Function around Ions.

Radial distribution functions (RDF) were computed to characterize molecular interactions in the aqueous systems. Six different systems were considered in these simulations, including Cl^+Cl^- , I^+I^- , NaI , I^+Na^- , LiI , and I^+Li^- aqueous solutions (see previous text for the description of notation). The RDFs of water for ions in Cl^+Cl^- and I^+I^- systems are shown in Figure 2a,b. It is seen from these RDFs that although in each system the positively and negatively charged ions have the same properties except for their charges, their interactions with water are quite different. In particular, the RDFs of water around the anions show more pronounced peaks and minima, indicating that the surrounding water molecules are better ordered than those around the cations. In the first solvation shell, water molecules approach closer to the anions than to the cations (as seen from the positions of the first peak of the water RDFs), again indicating tighter interactions between an individual anion with water at the first solvation shell than that between the corresponding cation and water molecules. This difference between cations and anions is the same for both the I^+I^- and Cl^+Cl^- systems, and the hydration of the smaller ions appears to be stronger than that of the larger ones with the same charge, showing an expected size-effect. It is interesting to note that although the charge density of Cl^+ is higher than I^- , the first peak of the RDF of the former is noticeably lower than that of the latter.

To further investigate the different hydration resulting from the change of the charge sign, we also performed MD simulations for two real systems, NaI and LiI , as well as for two corresponding artificial systems with signs of charges exchanged, I^+Na^- and I^+Li^- . (In order to check the RDFs obtained in this study, the RDF of water around I^- is compared to that of Dang et al.³⁷ simulations of NaI solution. The comparison shows that the RDFs calculated in the two simulations have good similarities. See Figure S7 in the Supporting Information.) As seen from the RDF of water around the ions, it is again clear that the change of the charge sign, with all other properties remaining the same, has a significant effect on the hydration of the charged particles. In all cases, anions tend to cause stronger ordering of the surrounding water molecules, and the first solvation shell of water is closer to the negative charges than to the corresponding positive ones. Both Na^- and Li^- strongly bind water molecules as seen from the high and sharp first peaks, and the effect, as expected, is stronger for the ion with the higher charge density. In contrast, the hydration shells of the corresponding cations are relatively loosely packed, as indicated by the broader and lower first

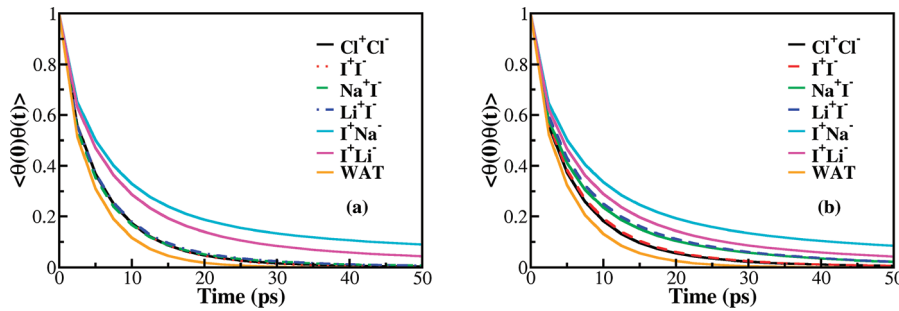


Figure 4. Rotational relaxation for (a) the O–H vector of water and (b) the dipole vector of water for the six different salt aqueous solutions compared with those of the pure water system.

Table 3. Fitting Parameters for the Rotational Relaxation of the O–H Vector

	A_1	τ_1 (ps)	A_2	τ_2 (ps)	A_3	τ_2 (ps)
I ⁺ Na ⁻	0.19	1.15	0.61	7.50	0.20	61.06
NaI ⁻	0.19	0.91	0.70	5.32	0.10	18.52
I ⁺ Li ⁻	0.19	1.10	0.63	7.07	0.18	34.33
Li ⁺ I ⁻	0.19	0.91	0.71	5.59	0.10	18.60
I ⁺ I ⁻	0.18	0.91	0.71	5.70	0.11	12.97
Cl ⁺ Cl ⁻	0.18	0.91	0.73	5.51	0.12	13.80

hydration shell peak and the weak structuring of water beyond the first solvation shells.

3.2. Effects of Counterions on the RDF of Water around Charged Particles. Next, we compare in Figure 3 the RDF of water around the same cation (anion) but with different counterions present in the solution. It is interesting to see from this figure that the change of the cation has relatively small effects on the peak positions of the RDF for the anion. The only noticeable difference is that the water RDF around I⁻ has a lower first peak when the cation is the artificial I⁺. As shown later, this peculiar behavior of I⁺I⁻ is likely a result of the strong ion-pairing in this system. In contrast, when the anion is changed, the peak positions of the water RDF around the cations can vary significantly, indicating a significant solvation shell structure change of the cation when the anion is changed from I⁻ to Na⁻ or Li⁻. In the former, a small peak appears at the position of minima for the latter two, ~5 Å, indicating the collapse of the second solvation shell onto the first one. These results again show that cation and anion hydration is intrinsically different from each other. The hydration of the anions is characterized by a strong anion–water association and is rather insensitive to the rest of the solvation environment, whereas the hydration of the cations is more diffusive and responds more readily to the change of the counterions. These differences in the solvation of cations and anions are more easily seen from their three-dimensional (3-D) distribution functions around water as discussed later [cf, Figures 8 and 9].

3.3. Ionic Effects on Dynamical Properties of Water. A number of experiments, including fs-IR, terahertz spectroscopy, and dielectric relaxation measurements, have been dedicated to characterize how inorganic salts affect the water rotational relaxation.^{39,44,45} These studies showed that in general the salt effects on water dynamics are complex and reflect largely the importance of ion cooperativity. In Figure 4a, we show the relaxation of the rotation of the O–H vector,

$$c_H(t) = \langle P_2[\vec{H}(t) \cdot \vec{H}(0)] \rangle \quad (1)$$

Table 4. Fitting Parameters for the Rotational Relaxation of the Water Dipole Vector

	A_1	τ_1 (ps)	A_2	τ_2 (ps)	A_3	τ_3 (ps)
I ⁺ Na ⁻	0.20	1.09	0.57	7.59	0.22	50.79
Na ⁺ I ⁻	0.20	0.93	0.56	5.42	0.24	20.55
Li ⁺ I ⁻	0.20	1.03	0.59	6.90	0.21	30.44
I ⁺ Li ⁻	0.19	0.90	0.56	5.61	0.25	20.20
I ⁺ I ⁻	0.20	0.95	0.69	5.98	0.11	17.30
Cl ⁺ Cl ⁻	0.19	0.94	0.70	5.76	0.10	17.50

where P_2 is the second order Legendre Polynomial, and \vec{H} stands for the O–H vector of the water molecule. In Figure 4b, we show the rotational relaxation of the dipole vector of water,

$$c_P(t) = \langle P_2[\vec{P}(t) \cdot \vec{P}(0)] \rangle \quad (2)$$

where \vec{P} stands for the vector of the water dipole (the unit vector pointing from the oxygen atom to the center of the line connecting the two hydrogen atoms). The average is over all water molecules near the center of the simulated water film and over the last 50 ns of the trajectories.

It is clearly seen from Figure 4 that the addition of salts can have noticeable effects on water relaxation, and the effects vary significantly with the type of ions present in the solution. In particular, the two systems with equal-sized anions and cations have the smallest effects on the rotational relaxation characterized by both O–H and dipole vectors of water. The two real systems, NaI and LiI, also have similar and small effects on the rotational relaxation of the O–H vector, but these salts significantly slow down the rotational relaxation of the water dipole vector. This difference in their effects on the O–H and dipole relaxation is consistent with their composition of large anions and small cations. As discussed by Bakker and co-workers,⁴⁵ anions and cations, due to their preferred interaction with the hydrogen and oxygen, respectively, mainly affect the O–H and dipole rotation, respectively. The small cations (especially Li⁺) interact strongly with the lone electron pair of the oxygen (represented by the negative charges at the center of the water molecule) and efficiently lock the dipole, whereas the larger anions have a weaker interaction with the positive charge, and the O–H rotation is less affected. The two artificial salts, I⁺Na⁻ and I⁺Li⁻, appear to strongly affect both relaxation times, with the former showing a slightly stronger effect. Their exceptionally strong effects appear to be related to the strong ion-pairing between the cations and anions, as discussed later.

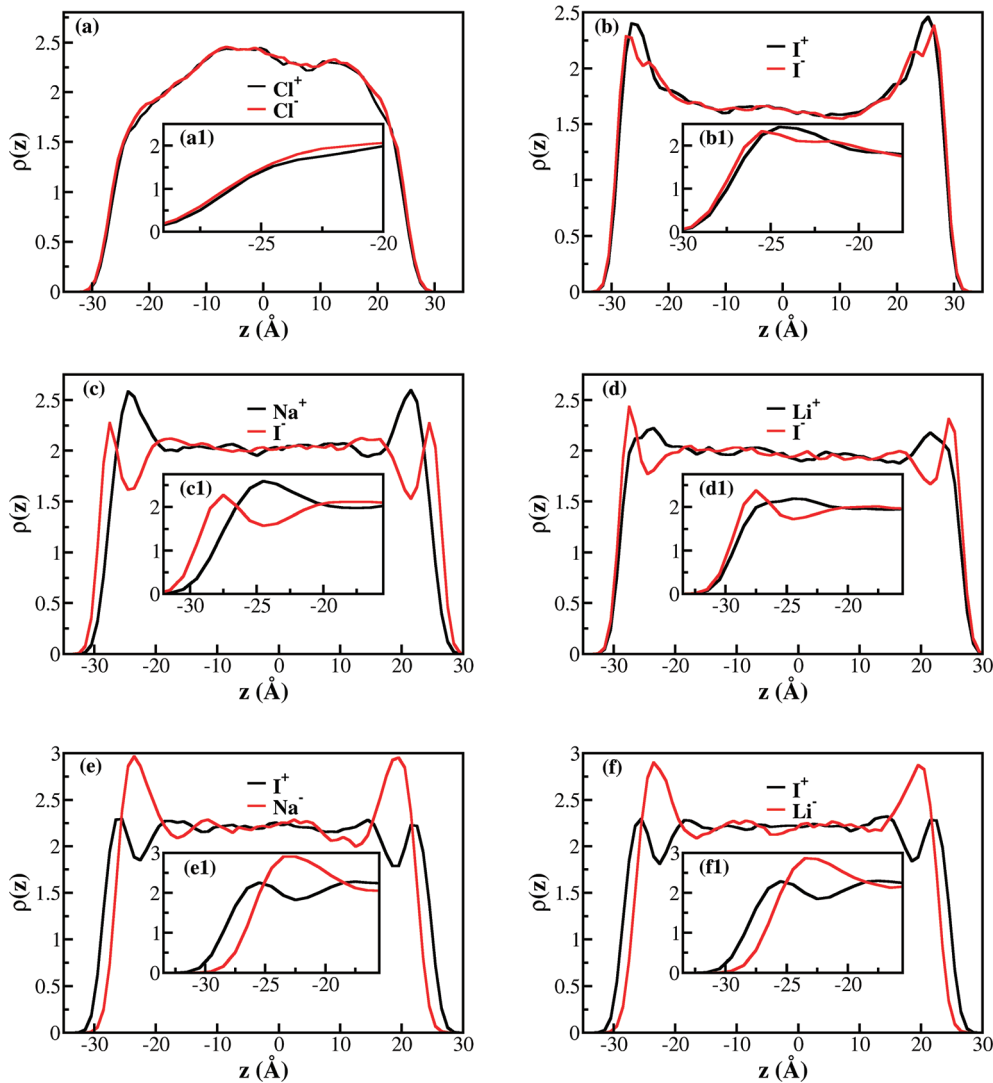


Figure 5. Distribution of ions across the simulation box and at the surfaces for the six different systems. (a) Cl^+Cl^- , (b) I^+I^- , (c) NaI , (d) LiI , (e) I^+Na^+ , and (f) I^+Li^+ .

To quantify the effects of the various salts on the rotational relaxation, we also fitted the curves given in Figure 4 by functions containing multiple exponentials. It was found that the fitting is satisfactory when three exponential terms are used (the fitted curves almost entirely overlap with the simulation data and are thus not shown):

$$c(t) = A_1 \exp(-t/\tau_1) + A_2 \exp(-t/\tau_2) + A_3 \exp(-t/\tau_3) \quad (3)$$

The fitting parameters are given in Table 3. Again, from this table it is clearly seen that the different combinations of anions and cations affect very differently the relaxation times, especially the long time behaviors, which are largely absent in pure water. Very slow relaxation was observed in Tables 3 and 4 for the two artificial systems and especially in the relaxation of the O–H vector, again suggesting other factors in influencing the observed time constants.

3.4. Surface Distribution of Charges. As seen from the above analyses, the intrinsic charge distribution of the SPC/E model used in the simulations results in different hydration of cations

and anions. In particular, from these analyses, the interactions between the anion and water molecules are more localized than that between the cations and water. The introduction of surfaces changes the solvation environment, and the dielectric constant at the surface is likely lower than that in the bulk. Since as mentioned above cations are more sensitive to the environment than anions, they are more likely affected by the surface, given that other conditions are the same. This is exactly what is seen for both I^+I^- and Cl^+Cl^- systems (Figure 5); the surface adsorption of anions are stronger than that of cations for both systems. The main difference between the two systems, that I^+ and I^- are enriched and Cl^+ and Cl^- are depleted at the surface, reflects the fact that with smaller sizes and thus higher charge density than the other pair, Cl^+ and Cl^- are better solvated in the bulk water. Since in this part of the simulation, fixed charge models were used, and as discussed later, strong ion-pairing exists between Cl^+ and Cl^- (see below), surface depletion instead of adsorption was observed for both the cation and anion.

The size effect in the surface adsorption of ions can also be seen from the other four systems (Figure 5) and is consistent with earlier studies. For example, the anions are largely enriched

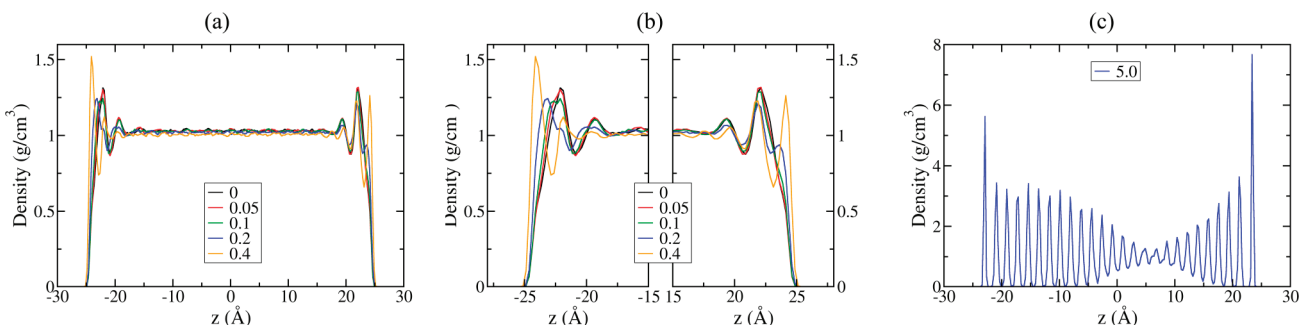


Figure 6. Density profile for water confined between positively (left, located at $\sim -25 \text{ \AA}$) and negatively (right, located at $\sim 25 \text{ \AA}$) charged surfaces: (a) the terminal charged atoms with 0, 0.005, 0.1, 0.2, and 0.4 unit charge, respectively; (b) scaled to show the surfaces in a; and (c) the terminal charged atoms with a 5.0 unit charge.

at the surface compared to the cations for NaI and LiI systems. However, after switching the sizes of the positively and negatively charged particles, for the artificial I^+Na^- and I^+Li^- systems, due to the much larger cation size, the cations instead of anions are preferentially adsorbed at the surface. However, it can be clearly seen from the comparison given in Figure 5 that although they are of the same size, again the surface concentration of I^- in NaI or LiI is higher than that of I^+ in I^+Na^- or I^+Li^- , further showing the difference in the solvation of positive and negative charges in these simulation systems. In summary, these results show that the size of the ions strongly affects their surface adsorption, at the same time the charge sign also plays an important role, with anions more likely occupying the surface.

3.5. Effects of Differently Charged Surfaces on the Structure of Water Confined in Between. From another point of view, we also used molecular dynamics simulations to investigate how surface charges affect the water structure. A similar simulation was performed by Luzar and co-workers.³² As seen from Figure 6, the surface charges do significantly affect the water distribution, and the effects manifest in a charge-sign-dependent manner. When the charge density is low, it is observed that the introduction of the negative charges to the confining surface induces a slight dewetting of the surface, which is counter-intuitive because one would expect that the introduction of the charges to the surface atoms will increase their hydrophilicity. These simulation results are consistent with earlier experiments and simulations.^{32,46,47} The introduction of positive charges, however, always promotes wetting of the otherwise hydrophobic surface. These results indicate that the introduction of negative charges with low charge densities would actually decrease the hydration of the particle and is consistent with the observation that anions but not cations tend to accumulate at the surfaces, indicating negatively charged particles with low charge densities interact less favorably than the positively charged ones.

When the surface charge density further increases (which would not be experimentally feasible but theoretically instructive), ordered structure layers form between the two confining surfaces, corresponding to the formation of cubic ice. The similar electrofreezing of confined water was also found by Zangi et al. in their molecular dynamics simulations of the confined TIPSP water model under the influence of a lateral external electric field, with a magnitude of 5 V/nm.⁴⁸ The interesting observation besides the electrofreezing in our simulations is that the first peak of water near the negatively charged surface is higher than that near the positively charged one. This result is again consistent with the

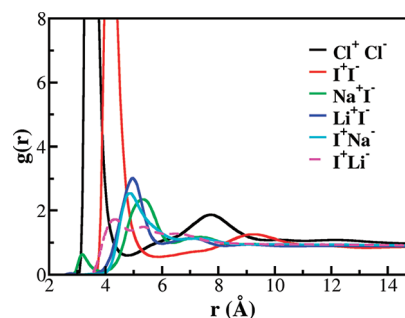
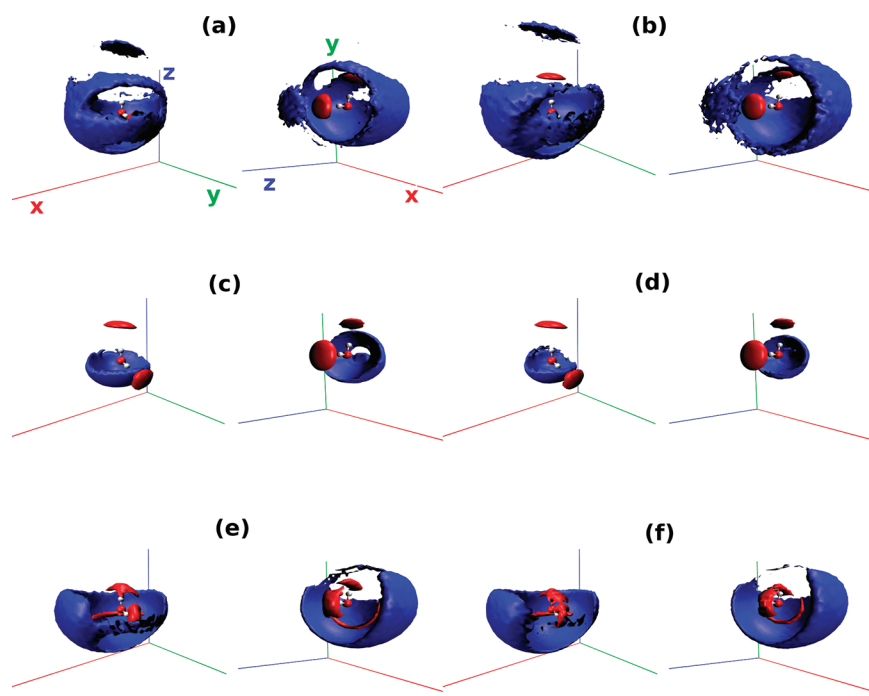


Figure 7. RDF of cations around the central anions for the different systems.

earlier assessment of the hydration of anions and cations: negative charges have a higher tendency of ordering the first solvation shell water molecules, especially at high charge densities. Therefore, the effects of charged surfaces on the water structure are consistent with the effects of the solvated charged particles on the nearby water structure and strongly indicate that, at least for the water models used, there is a significant difference between the hydration of positive and negative charges.

3.6. Ion–Ion Radial Distribution Functions. Next, to characterize charge–charge interactions, we calculated the radial distribution functions between the oppositely charged particles. Although the radii of the $\text{I}^+(\text{I}^-)$ and $\text{Cl}^+(\text{Cl}^-)$ are quite different from each other, their ion–ion distribution functions are rather similar. The only difference between them is the higher peak for the Cl^+Cl^- than for the other system, reflecting the fact that Cl^+ and Cl^- have higher charge densities than I^+ and I^- . Both systems show a pronounced peak at a distance corresponding to the direct contact between a pair of ions (which resulted in a CIP, contact ion pair⁴⁹) is much less likely to be observed for systems with different cation and anion sizes. The RDF of the latter systems (all four of them) lacks the high peak at the distance of the direct contact position and shows high peaks at a longer distance, suggesting the formation of ion pairs that are not in direct contact. As a result, in the systems of ions of the same size it is easy to form direct ion pairs, and thus, the counterions occupy significantly the first solvation shell of the ion and reduces its hydration (see Figure 3).

Within the four systems with unequal cation and anion sizes, there are also significant differences. First, the highest peaks for the two artificially charged systems (I^+Na^- and I^+Li^-) are at a



13

Figure 8. Three-dimensional distribution function of ions surrounding water (aligned to the same configuration that the oxygen is at (0,0,0), one O–H pointing to the positive direction of the z -axis, and the other O–H in the left down corner of the x – z plane. (a) Cl^+Cl^- , (b) I^+I^- , (c) NaI , (d) LiI , (e) I^+Na^+ , and (f) I^+Li^- .

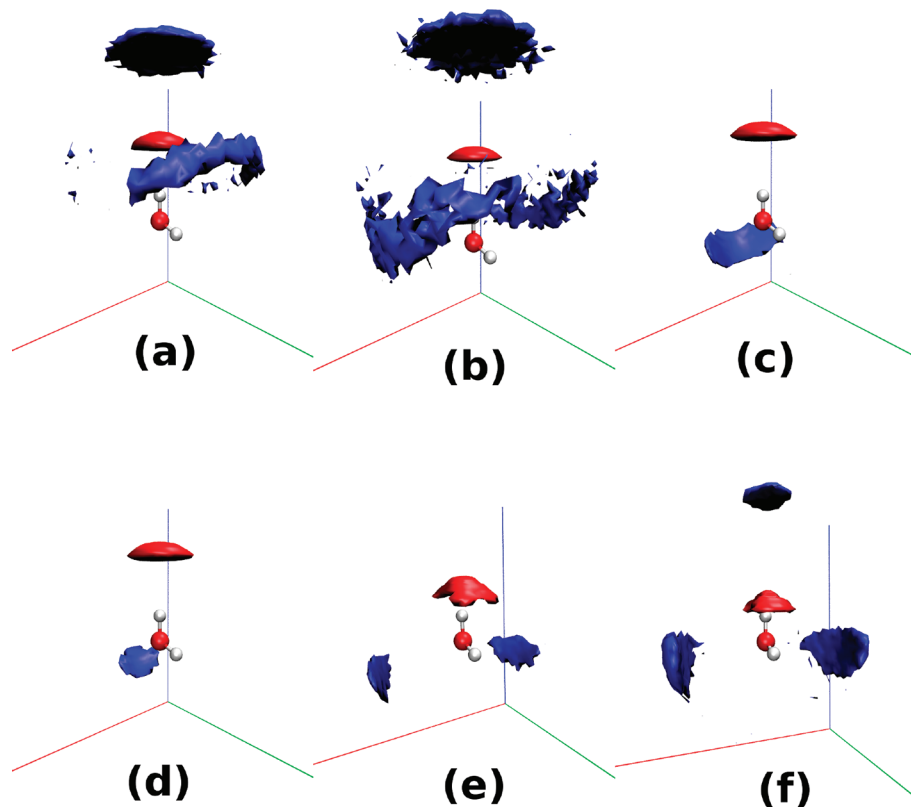


Figure 9. Similar to Figure 8, but for the subpopulation at which one anion is located near the hydrogen pointing upward.

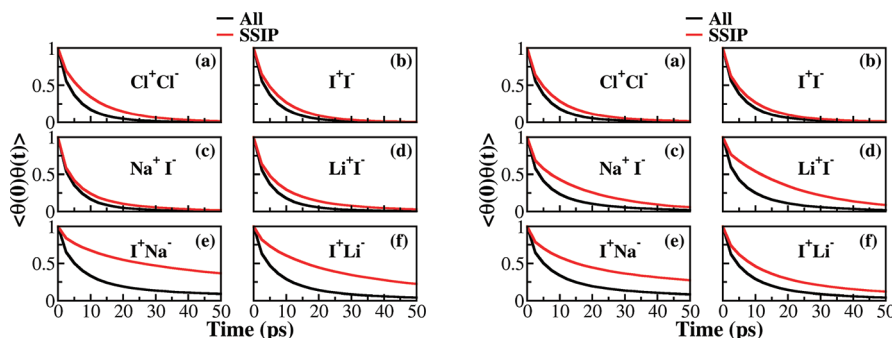


Figure 10. Comparison of rotational relaxation for the central water molecules in SSIP and the entire population. The six figures on the left show the rotational relaxation for the O–H vector of water, and the six figures on the right show the rotational relaxation for the dipole vector of water.

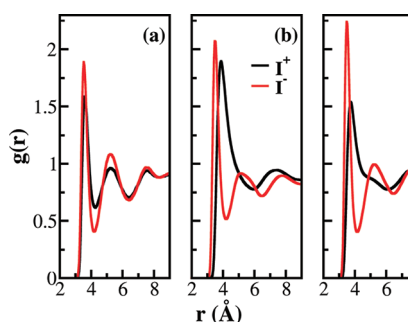


Figure 11. RDF of different types of water molecules surrounding I^+ and I^- . (a) TIPSP, (b) POL3, and (c) SPC/E.

shorter distance than that of the two corresponding normal systems (NaI and LiI), indicating a tighter (although not direct either) ion-pairing in the former systems. We should note here that the sum of the van der Waals radius is the same for I^+Na^- and NaI , as well as for I^+Li^- and LiI . Second, the direct contact peak (at about 3.1 Å for NaI and 2.7 Å for LiI ; see Figure 3) is higher for NaI and LiI . If we take into account the I^+I^- system, one sees that as the difference between the cation and anion sizes increases, it becomes more difficult for the direct ion pair to form, consistent with the rule of matching water affinity. The same trend can also be seen for the I^+I^- , I^+Na^- , and I^+Li^- series. For the species I^+Li^- , one does not observe a direct contact ion pair from examining its ion–ion RDF diagram, and for the systems I^+I^- and I^+Na^- , the height of the first indirect peak ($\text{I}^+\text{I}^- > \text{I}^+\text{Na}^-$) is also consistent with the argument that the formation of ion pairs becomes more difficult for systems with bigger cation–anion solvation energy differences.

To better understand the ion-pairing in the systems discussed above, we also plotted 3-D distribution profiles (Figure 8). In these figures, the center water molecule is positioned at a fixed configuration, with one hydrogen atom pointing to the positive z -direction. We then search for the configurations in which there is an anion in direct contact (the distance between the anion and the oxygen atom of the water molecule is equal to or less than the radius of the anion's first solvation shell, and the anion must be at the positive direction of the system's z -axis) with the central water molecule. Finally, for such water–anion configurations, the probability distribution of the cations and anions are calculated and shown in 3-D diagrams (Figure 9). It is clearly seen from these figures that ion distributions are significantly different between systems of similar positive and negative ion (as the

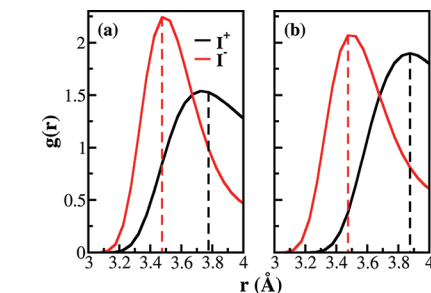


Figure 12. RDF of different types of water molecules surrounding I^+ and I^- . Here, only the first peaks are shown to clarify the differences between the two water models: (a) SPC/E and (b) POL3.

artificial systems I^+I^- and Cl^+Cl^-) sizes and those with different sizes. Consistent with the previously shown RDF, both I^+I^- and Cl^+Cl^- systems are characterized by close cation and anion contacts (CIP), whereas all other four systems show highly populated structures with cations and anions arranged roughly at the tetrahedral corners of the center water. Therefore, these figures confirm that the highest peaks in the RDFs (Figure 7) for NaI , LiI , I^+Na^- , and I^+Li^- correspond to the single solvent separated ion pairs (SSIP).

Combining the RDF and the 3-D distribution function diagrams, a simple explanation of the effects of various salts on the rotational relaxation can now be obtained. First, I^+Na^- and I^+Li^- form favorable SSIP in which the bridging water molecule is locked between the cation and anion. As a result, it is expected that the rotation of these water molecules, measured by the rotational relaxation of the O–H or the dipole vector, is significantly slowed down. Of the above two systems, I^+Na^- shows a higher SSIP peak than I^+Li^- and correspondingly has a stronger retarding effect for the water rotation. The I^+I^- and Cl^+Cl^- systems mainly form direct ion pairs but not SSIP and thus have relatively small effects on water relaxation (no significant locking of water molecules but a pair or pairs of cations and anions). To further validate the argument that SSIPs tend to generate slow rotating water molecules, we further selected water molecules that have at least one pair of cation and anion at its tetrahedral positions and calculated their rotational relaxation. As seen in Figure 10, the rotational relaxation of such water molecules is significantly slower than that calculated for the entire population.

The NaI and LiI systems also form more SSIP than CIP (although they have higher probabilities of CIP formation than I^+Na^- and

I^+Li^- , respectively). The SSIP in these systems also appear to have slightly different structures from those in the I^+Na^- and I^+Li^- systems. As discussed earlier, their ion pairs are less compact, and their effects on the rotational relaxation of water are weaker than I^+Na^- and I^+Li^- . Especially, the large I^- has a low charge density and interacts weakly with water (which can also be seen from its preferred surface adsorption). Therefore, they have a negligible effect on the rotation of the O–H vector of water. Their cations, however, are small and have strong effects on the rotation of the water dipole vector.

4. CONCLUSIONS

In this article, we utilized the advantages of MD simulations in testing theoretical models by artificially modified force field parameters to study how the charge sign and van der Waals radius affect the hydration of charged particles in aqueous solutions. It has been argued that both size and polarizability noticeably affect solvation and distribution of ions at the surfaces. To simplify the picture, most of the simulations were performed in the study using the fixed charge models, in particular the SPC/E model for water and the AMBER general force field for ions. Besides the two normal systems, NaI and LiI, we designed four artificial systems, Cl^+Cl^- , I^+I^- , I^+Na^- , and I^+Li^- . Simulations performed on these systems all indicate that the hydration of cations are different from that of anions, even when other properties (such as the radius) of the ions are the same. In the hydration of anions, water molecules can approach closer to the ion, presumably as a result of the positive charge carried by the hydrogen being closer to the periphery of the water molecule and allows for stronger electrostatic interaction between the anions and water. The anion–water interaction is thus also more local in that the first peak of the water RDF around an anion is sharper than that around a cation, as well as in that the angular distribution of anions around water molecules is narrower than cations. The nearest cations around water, although do not approach water as closely as anions do, have a broader radial and angular distribution around water. They are expelled to a larger extent than anions from the surface. The ionic radius, consistent with earlier studies, was also shown to have a strong influence on the ion adsorption: the larger ions are more likely to populate at the surfaces. Since the current simulations were performed with very simple fixed point charge models, the origin of the observed different behaviors of charged particles with all identical properties except for the charge sign must lie in the charge asymmetry of the water model used. For example, in the SPC/E model, the negative charge is closer to the center of the molecule than the two positive partial charges carried at the two hydrogen atoms. As a result, although each of the positive charges have only half of the magnitude of the negative one, anions can approach closer to the positive charges of water than the cations do to the negative charge located at the oxygen atom. The charge distribution of the water molecule was shown in an earlier analysis to be responsible for the preferred orientation of water molecules at water/air interfaces.²⁸

However, it is also important to note that the difference between the surface distributions of positively and negatively charged otherwise identical particles is small, when compared to systems with different sizes of ions. As pointed out earlier, polarizability might also play an important role,^{5,20,25} although recent water–ion and ion–ion interacting analyses show the difficulty and possible pitfalls in separating the size and polarizability effects.⁴⁴ The current study

focuses on testing how the change of the charge signs affects their properties calculated using the specified water models but not on the ion surface distributions of real salt aqueous solution systems.

To test the effect of point charge distributions and polarizability on the hydration of ions, we also performed MD simulations using the TIPSP water model and the POL3 polarizable force field for the I^+I^- system. Figure 11a shows that the difference between the hydration of the cation and that of the anion becomes small (the positions of the first and second peaks and valleys are almost identical, although the peak heights are different) when the TIPSP water model is used. This result is expected since the positive and negative charges are more symmetrically distributed in this water model, which largely removes the differences in cation/anion–water interactions. The difference between results obtained using the SPC/E and TIPSP water models suggests that one should be careful about the choice of water models in studying the solvation of charges in water. These results also further demonstrate that, at least at this simulation level, the intrinsic charge distribution of the SPC/E water model is responsible for the different behaviors of positively and negatively charged particles. The simulation using the polarizable force field, however, yields results that are similar to that obtained using the SPC/E model with an even stronger difference between anion and cation hydration (the positions of the first peaks for the cation and anion are separated even more; see Figure 11b,c and 12), further showing the importance of charge asymmetry in ion solvation. The three water models show the following order: TIPSP < SPC/E < POL3, in terms of the increasing capability of differentiating cation and anion hydration.

The differences in the hydration of cations and anions in turn affect their association in water. Besides the expected matching water effect, which favors ion-pairing (in particular CIP) between ions with similar sizes, it was also found that the switch of the charge signs between the cation and the anion has a rather strong effect on ion association and consequently on the rotational relaxation of water molecules. Ranking of the systems based on their capability of forming direct ion pairs gives $\text{Cl}^+\text{Cl}^- > \text{I}^+\text{I}^- > \text{NaI} > \text{LiI} > \text{I}^+\text{Na}^- > \text{I}^+\text{Li}^-$. This trend is consistent with the argument that ion-pairing occurs following the rule of matching water affinity. The systems with the same anion and cation sizes are the most likely to form direct pairs, and the stronger trend of Cl^+Cl^- than that of I^+I^- in forming ion pairs, however, reflects the effect of a higher charge density. Furthermore, the direct ion-pairing is stronger for the normal systems, NaI and LiI, than that for the correspondingly inversely charged systems, again indicating the difference in the hydration of cations and anions. However, one surprising finding of the present article is that the extent of ion-pairing does not correlate directly to the effects of ions on water dynamics. Direct ion-pairing, in fact, tends to have a small effect on water rotational relaxation, which is mostly significantly slowed down as a result of the well structured single solvent separated ion pairs. The current study thus suggests that the relationship between water dynamics and structural information could be complicated, and caution is needed for the interpretation of water dynamics data based on simple structural models.

These simulations indicate the importance of the charge distribution in water in distinguishing the positive and negative charges through different hydration. The latter in turn affects rather strongly other properties, such as water dynamics, and probably also the solvation capability of water, and thus shows the importance of using

appropriate charge models of water (TIPSP shows a very different behavior from SPC/E). The examination of the real physical significance of the current study certainly relies on carefully designed experiments but would also depend on accurate first principle calculations.

■ ASSOCIATED CONTENT

S Supporting Information. The results of the simulation using the cutoff of 13 Å for the Li^+I^- /water solution slab and those of the simulation using the grid spacing of 0.5 Å for the Li^+I^- /water solution slab. This material is available free of charge via the Internet at <http://pubs.acs.org.org>.

■ AUTHOR INFORMATION

Corresponding Author

*Phone: 86-10-62752431. E-mail: gaoyq@pku.edu.cn.

■ ACKNOWLEDGMENT

We thank the National Natural Science Foundation of China (L.Y., 21003004; Y.Q.G., 91027044) and the Chinese Ministry of Education (L.Y., 20100001120015; Y.Q.G., 20100001110024) for financial support. Y.Q.G. is also a 2008 Changjiang Scholar of Chinese Ministry of Education. The project was also partly supported by Peking University. Computer resources were provided by the Shanghai Supercomputer Center of China.

■ REFERENCES

- (1) Shen, Y. R.; Ostroverkhov, V. *Chem. Rev.* **2006**, *106*, 1140.
- (2) Kuo, I. F. W.; Mundy, C. J. *Science* **2004**, *303*, 658.
- (3) Baldwin, R. L. *Biophys. J.* **1996**, *71*, 2056.
- (4) Arakawa, T.; Timasheff, S. N. *Biochemistry* **1982**, *21*, 6545.
- (5) Jungwirth, P.; Tobias, D. J. *Chem. Rev.* **2006**, *106*, 1259.
- (6) Pegram, L. M.; Record, M. T. *J. Phys. Chem. B* **2007**, *111*, 5411.
- (7) Bakker, H. J.; Tielrooij, K. J.; Garcia-Araez, N.; Bonn, M. *Science* **2010**, *328*, 1006.
- (8) Jungwirth, P.; Winter, B. *Annu. Rev. Phys. Chem.* **2008**, *59*, 343.
- (9) Tobias, D. J.; Brown, M. A.; D'Auria, R.; Kuo, I. F. W.; Krisch, M. J.; Starr, D. E.; Bluhm, H.; Hemminger, J. C. *Phys. Chem. Chem. Phys.* **2008**, *10*, 4778.
- (10) Jungwirth, P.; Ghosal, S.; Brown, M. A.; Bluhm, H.; Krisch, M. J.; Salmeron, M.; Hemminger, J. C. *J. Phys. Chem. A* **2008**, *112*, 12378.
- (11) Fennell, C. J.; Bizjak, A.; Vlachy, V.; Dill, K. A. *J. Phys. Chem. B* **2009**, *113*, 6782.
- (12) Levin, Y. *Phys. Rev. Lett.* **2009**, *102*.
- (13) Baldelli, S.; Santos, C. S. *Chem. Soc. Rev.* **2010**, *39*, 2136.
- (14) Record, M. T.; Zhang, W. T.; Anderson, C. F. *Adv. Protein Chem.* **1998**, *51*, 281.
- (15) Pegram, L. M.; Record, M. T. *Proc. Natl. Acad. Sci. U.S.A.* **2006**, *103*, 14278.
- (16) Jungwirth, P.; Tobias, D. J. *J. Phys. Chem. B* **2001**, *105*, 10468.
- (17) Kuo, I. F. W.; Mundy, C. J.; Eggimann, B. L.; McGrath, M. J.; Siepmann, J. I.; Chen, B.; Vieceli, J.; Tobias, D. J. *J. Phys. Chem. B* **2006**, *110*, 3738.
- (18) Winter, B.; Faubel, M.; Vacha, R.; Jungwirth, P. *Chem. Phys. Lett.* **2009**, *474*, 241.
- (19) Smith, J. D.; Saykally, R. J.; Geissler, P. L. *J. Am. Chem. Soc.* **2007**, *129*, 13847.
- (20) Wick, C. D.; Dang, L. X. *J. Chem. Phys.* **2010**, *132*, 044702.
- (21) Petersen, P. B.; Saykally, R. J. *J. Chem. Phys. Lett.* **2004**, *397*, 51.
- (22) Buyukdagli, S.; Achim, C. V.; Ala-Nissila, T. *J. Stat. Mech.: Theory Exp.* **2011**, 05033.
- (23) Zhang, Y. J.; Cremer, P. S. *Annu. Rev. Phys. Chem.* **2010**, *61*, 63.
- (24) Marcus, Y. *Chem. Rev.* **2009**, *109*, 1346.
- (25) Wick, C. D.; Kuo, I. F. W.; Mundy, C. J.; Dang, L. X. *J. Chem. Theory Comput.* **2007**, *3*, 2002.
- (26) Lee, C. Y.; Mccammon, J. A.; Rossky, P. J. *J. Chem. Phys.* **1984**, *80*, 4448.
- (27) Morita, A.; Hynes, J. T. *Chem. Phys.* **2000**, *258*, 371.
- (28) Fan, Y. B.; Chen, X.; Yang, L. J.; Cremer, P. S.; Gao, Y. Q. *J. Phys. Chem. B* **2009**, *113*, 11672.
- (29) Leung, K. *J. Phys. Chem. Lett.* **2010**, *1*, 496.
- (30) Kathmann, S. M.; Kuo, I. F. W.; Mundy, C. J.; Schenter, G. K. *J. Phys. Chem. B* **2011**, *115*, 4369.
- (31) Vaitheeswaran, S.; Thirumalai, D. *J. Am. Chem. Soc.* **2006**, *128*, 13490.
- (32) Bratko, D.; Daub, C. D.; Leung, K.; Luzar, A. *J. Am. Chem. Soc.* **2007**, *129*, 2504.
- (33) Joung, I. S.; Cheatham, T. E. *J. Phys. Chem. B* **2008**, *112*, 9020.
- (34) Mahoney, M. W.; Jorgensen, W. L. *J. Chem. Phys.* **2000**, *112*, 8910.
- (35) Caldwell, J. W.; Kollman, P. A. *J. Phys. Chem.* **1995**, *99*, 6208.
- (36) Dang, L. X.; Chang, T. M. *J. Chem. Phys.* **1997**, *106*, 8149.
- (37) Dang, L. X. *J. Phys. Chem. B* **2002**, *106*, 10388.
- (38) Case, D. A.; Darden, T. A.; Cheatham, T. E.; et al.; AMBER9; University of California: San Francisco, 2006.
- (39) Darden, T.; York, D.; Pedersen, L. *J. Chem. Phys.* **1993**, *98*, 10089.
- (40) Trokhymchuk, A.; Alejandre, J. *J. Chem. Phys.* **1999**, *111*, 8510.
- (41) Frenkel, D.; Smit, B. *Understanding Molecular Simulation: From Algorithms to Applications*; Academic Press: San Diego, CA, 1996.
- (42) Janecek, J. *J. Phys. Chem. B* **2006**, *110*, 6264.
- (43) Alejandre, J.; Tildesley, D. J.; Chapela, G. A. *J. Chem. Phys.* **1995**, *102*, 4574.
- (44) Caleman, C.; Hub, J. S.; van Maaren, P. J.; van der Spoel, D. *Proc. Natl. Acad. Sci. U.S.A.* **2011**, *108*, 6838.
- (45) Tielrooij, K. J.; Garcia-Araez, N.; Bonn, M.; Bakker, H. J. *Science* **2010**, *328*, 1006.
- (46) Zhang, X. Y.; Zhu, Y. X.; Granick, S. *J. Am. Chem. Soc.* **2001**, *123*, 6736.
- (47) Zhang, X. Y.; Zhu, Y. X.; Granick, S. *Science* **2002**, *295*, 663.
- (48) Zangi, R.; Mark, A. E. *J. Chem. Phys.* **2004**, *120*, 7123.
- (49) Buchner, R.; Capewell, S. G.; Heft, G.; May, P. M. *J. Phys. Chem. B* **1999**, *103*, 1185.